Journal of Thermal Analysis and Calorimetry, Vol. 81 (2005) 489–500

ON THE MORE INFORMATIVE VERSION OF THERMOMECHANICAL ANALYSIS AT COMPRESSION MODE
A review

Y. A. Olkhov[1] *and B. Jurkowski*[2*]

[1]Institute of the Problems of Chemical Physics, Russian Academy of Sciences, 142 432 Chernogolovka, Moscow Region, Russia,
[2]Plastic and Rubber Processing Division, Institute of Materials Technology, Poznan University of Technology, Piotrowo 3, 61-138 Poznan, Poland

An adjusted version of description of some characteristics of linear, crosslinked, and filled polymers by using a more informative version of TMA at a compression mode is presented. It is based on a model network with physical and/or chemical junctions and testing a layer up to 0.5 mm thick of polymers in rigid and viscoelastic states. The TMA makes possible to describe a structure with two or three topological regions exhibiting various relaxation transition temperatures, the difference is up to 200°C. This method makes possible to evaluate also characteristics of molecular mass distribution of the chain segments between branching junctions in particular regions, crystallinity degree, and compactness. Knowledge of these properties helps an optimization of formulation of the polymeric material and processing technology. In this work, changes in previous definitions are introduced, too.

Keywords: *correlation, crystallinity degree, MMD between junctions, molecular structure, nanocomposite, relaxation transitions, temporary network, topological structure*

Introduction

Polymers behave as a network, independently on a fact, whether they are linear or cross-linked, but the properties of the networks differ. The difference is that the end of mechanical relaxation process, recorded at high temperature by TMA, means the beginning of flow or a plateau of the high-elasticity for linear or cross-linked polymers, respectively. Structural elements present in the material reveal a spectrum of interaction energies [1, 2]. This allows characterizing the structure of multi-component and/or multi-phase systems in a simpler way, by using some composed values, than if a full analysis on a molecular level is performed. For this purpose, the values averaging the effects of action of the structural elements on the thermomechanical properties of the material could be used.

The polymer network is assumed as a system with physical or physical and chemical branching junctions. The typical chains may be 1 μm–1 mm in a contour length causing that a single chain may participate in several metastable mesophases [3–5] having a size range from 1 to 50 nm [6], when the domains of amorphous phase have often dimensions in nanometers [7].

Determination of MMD in the cross-linked polymer is possible by using spectra of boiling or crystallization temperatures of the solvent occluded in the swollen polymer, or stress relaxation times or solvent freezing point depression, and high-temperature NMR [8–13]. However, these methods give the relative values of the chain length [14, 15]. Relationships between properties of polymers in rigid or visco-elastic physical states and molecular mass (MM) or/and MMD have been widely discussed [16–21]. For such studies one should postulate or experimentally determine relationships between a spectrum of relaxation times, or other relaxation characteristics like viscosity or temperature of the beginning of flow (T_f) at accepted measuring conditions and MM of a particular fraction of the chains [16].

The constants characterizing Baumgartel– Schausberger–Winter (BSW)-spectrum, which represents the precursor of relaxation behavior for monodispersive linear polymers, and selection of relaxation times [22] also have insufficient theoretical basis [16]. The domains of long-range order could be considered to be distinctly influencing the arrangement of the chains present in the amorphous phase. This results in the appearance of two amorphous regions in the system. First behaves a typical amorphous structure, whereas the second one as intermediate between amorphous and crystalline. The unperturbed amorphous structure exhibits transition at T_g (DSC) and a single discrete peak (DMTA, DETA, TMA) often also accepted as a measure of location of T_g. Several relaxation transitions are found when the system contains the crystals distributed within the amor-

* Author for correspondence: boleslaw.jurkowski@put.poznan.pl

1388–6150/$20.00

Akadémiai Kiadó, Budapest, Hungary
Springer, Dordrecht, The Netherlands

phous phase [23–25]. It causes variation in properties of the amorphous phase, especially at mesophases.

In this work, idea of more informative version of TMA [26, 27] is discussed and compared with literature. This method makes possible to discriminate in polymers two or three topological regions exhibiting various relaxation transitions and to evaluate characteristics of MMD of the chain segments between physical and chemical branching junctions of a network in particular regions. Knowing them and anisotropy of local properties, and specimen crystallinity degree, all evaluated by a single TMA test, should help to optimize the formulation of the polymeric material and processing technology.

General aspects of investigations at compression mode

Mechanical methods are sensitive to relaxation transitions [28]. TMA is based on measurements of the specimen deformation, which was acquired under very low load (Fig. 1), as a function of scanned temperature giving a thermomechanical curve (TMC) [29]. The TMC could be approximated as lines with several breaks separating the apparently linear segments with varied slopes, what informs about an existence of material regions with different thermal expansion properties. These regions differ in degree of order or interaction energies. Thus, the TMC may be used to characterize quantitatively a polymer topological structure; it means regions having complex associated structures with higher-level organization than the molecular one. Architecture with two or three amorphous regions (e.g., in the volume between adjacent lamellae), probably interpenetrating is found. These regions are not divided in space; they represent several types of interactions, which coexist in polymers. However, from TMC, it is impossible to discriminate particular interactions existed on the molecular level.

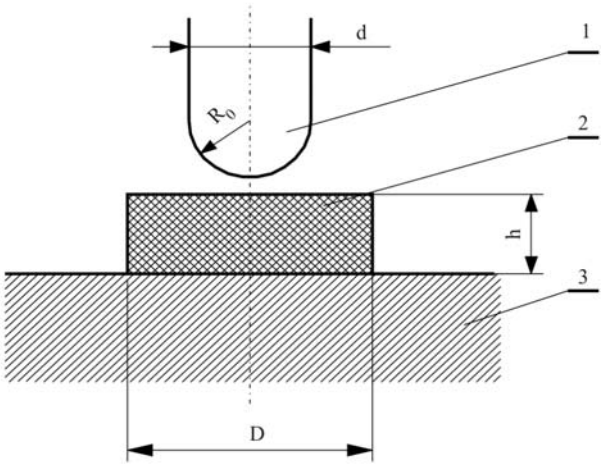

Fig. 1 Schematic illustration of the TMA device: 1 – probe hemispherical tip, 2 – specimen, 3 – base

TMA usually measures polymer properties in a layer up to 0.5 mm thick, but if the radius of the probe tip penetrating the specimen is increased from 1 to 5 mm, this thickness will grow up to 2.5 mm [30]. To ensure reversibility, the initial deformation H (obeying a Hooke's law) applied to the polymer is below 0.05 mm.

The glass transition temperature T_g is influenced by supermolecular structure (still controversial problem) changing at polymer testing. Thermomechanical contribution is dominant in the microthermal response of polymers due to a variable physical contact area for the TMA probe tip [31]. For this reason, T_g (defined in a different way by different authors) determined by DETA and DMTA that recording local and structural relaxation that depends on the thermal and stress history of the specimen as well as the loading rate or frequency at measurement [32]. It is different from T_g^{DSC} which is the phase transition temperature reflecting a change in entropy. The T_g^{TMA} reflects mechanical relaxation, but *o*ften it accords sufficiently well with those determined by other methods [33–35].

The thermal expansion coefficient [36], the softening temperature [37], the cross-linking degree from equilibrium elastic modulus [38, 39], and the average number of degrees of freedom of the chain segments between cross-links [40] could be evaluated by TMA. Therefore, it is used in the industry [41], but usually for comparative tests.

The individual components of the polymer network cannot be identified by TMA. The temperature of the beginning of flow, T_f, for linear polymers can be identified as a condition of gel transition [42]. It means a process of the physical network degradation runs that undertake testing conditions (stress, a rate of loading) at the temperature $\geq T_f$. The transition from rubber-like equilibrium gel to liquid needs rather long time. The viscosity, the number and size of clusters, a correlation length of the cluster (proportional to its diameter) prior to reaching the gel point, and the equilibrium elastic modulus are stable for each conversion degree [43]. All these suggest [44, 45] that the transitional zone on TMC (Fig. 2, shaded area), reflects a pseudo-integral function of MMD of the chain segments between junctions in the polymer network.

Termination of the segmental relaxation is revealed in the system, which is under certain loading, as a jump in deformation ΔH (measured as a change in height of the specimen) that is directly proportional to the mass fraction of the involved molecules. In view of this, the transitional zone can be represented as an envelope of deformation jumps (Fig. 2). If it is true, TMC evaluated under special conditions is an apparent equi-

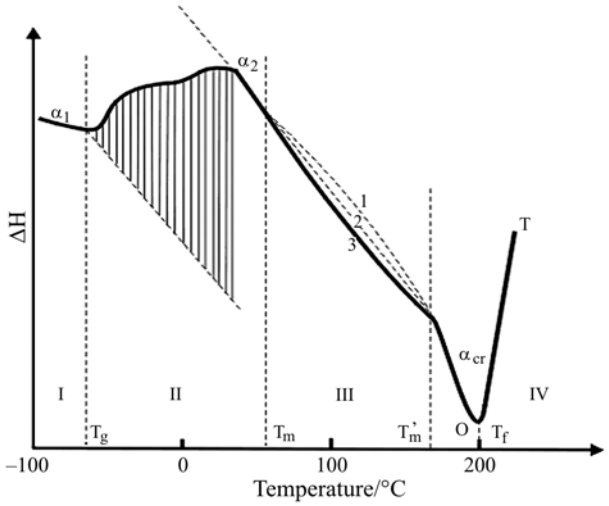

Fig. 2 Thermomechanical curve for PA6 that before testing has passed through the single screw extruder and the static mixer with holes 1.9 mm in diameter: I – glassy state, II – rubbery state of the amorphous region, III – crystalline zone, IV – melting of the crystalline portion, 1, 2 and 3 – variants of the transition process, α_1 – linear thermal expansion coefficient for a glassy state of amorphous region, α_2 – linear thermal expansion coefficient for a rubbery state of amorphous region and α_{cr} – coefficient of the thermal change in linear dimensions during melting; for this curve α_2/α_1=3.2 and α_{cr}/α_1=8.9

librium and can be used for the analysis of MMD of the chain segments between the physical junctions for linear polymers or between the physical junctions and cross-links for cross-linked polymers. However, a certain role of the *P*/*E* parameter is observed for the obtained results (*P* is the stress and *E* is the elastic modulus). This implies that TMC for any system depends on the MMD and on time-dependent structural parameters, which determine the material deformability [46].

The MM of the chain segments between junctions of the physical network at a temperature close to T_g, for amorphous polymer, or T_m, for crystalline one, equals the Kuhn segment [47]. This fact agrees with devitrification of the segmental mobility of the chain segments those exceed the Kuhn segment [47–49]. The glass transition can be found by measuring the thermal expansion rates for the glassy and rubbery states.

Semi-crystalline polymers with MM>10000 g mol^{-1} in the solid state are globally metastable and divided into microphases and nanophases with strong, covalent bonds crossing the phase boundaries. The segments of larger molecules that can move independently, i.e. which are decoupled from the rest of the chain, also can crystallize and melt reversibly and resemble the corresponding, independent, small molecules [50].

The glasses may have structures corresponding to liquids or mesophases and can exist [51] as a rigid-amorphous fraction (RAF). A multilevel structure with mesophases does not allow a fast melting below the T_g and hinders recrystallization [51]. Simultaneously, RAF could increase as the crystallinity increases and is not part of secondary crystallization only [52]. The disappearance of RAF on melting could go parallel with the disappearance of the molten crystals. The material containing both amorphous and partially ordered structures [53–55] causes rather unique properties, which vary with the thermal and mechanical history of the specimen.

Apparently, the higher probability to identify the interactions between chains as physical junctions, the more accurate is the interpretation of the experimental data within the framework of this approach, as it was described for a system with strong hydrogen bonds, clusters, etc. [56–58].

Relationships between molecular mass and flow temperature

For low-MM linear polymers, T_m and T_g rise with MM [59–61]. However, there is a limit to this behavior (as is a case of high-MM linear polymer [62] or cross-linked rubber [45], when such correlation is absent), as even the limited conformational changes in a rigid mesogen will contribute enough entropy to prevent the T_m from growing indefinitely [61].

A polymer melt will become more viscous with increasing MM, especially, when chain entanglements limit molecular motions [61]. Some relationships between $\Delta T=T_f-T_g$ or T_f and the MM of a polymer homologue proceeding from the effect of the MM on its viscosity are known [16–21]. A criterion for the transition from rubbery state to a viscous flow expressed by the thermomechanical curve (TMC) could be the beginning of the growth in the derivative of deformation d*H* with respect to the temperature d*H*/d*T*. The observed increase in d*H*/d*T* may result from a sharp drop in the elastic modulus, caused by the temperature-induced degradation of the physical branching junctions [46]. Hence, the method implies an evaluation of two properties of the chains in a thermal field within a specimen that varies with time. Firstly, segmental relaxation starts at T_g or T_m and it ends when the lowest MM polymer homologue starts to flow at T_f that corresponds to the *O* point, Fig. 2 (minimum on the curve). At this point, the elastic modulus for the polymer approaches a value resulted from both the thermal expansion and resistance to flow by the chain entanglements (the curve *OT*). However, a polydispersive polymer at this temperature would not flow under processing conditions. For proper process-

ing it is required a higher temperature be reached to ensure technological flow at a given shear rate, at which the highest MM polymer fractions start to flow. Because of this phenomenon, for a given polymer, the wider MMD, the higher the processing temperature is. An increase in specimen deformation, H, at temperatures $>T_f$ gives evidence that thermal expansion is higher than deformation caused by a small load, applied on a probe of a TMA device.

Thermomechanical deformation is terminating due to stabilization of the elastic modulus, and the polymer reaches the plateau of the high-elasticity [63]. The higher MM of a polymer homologue between junctions, the higher is the temperature when the plateau is reached. This rule can be described by the empirical equation [46], similarly to the classical Williams–Landel–Ferry equation [64], as follows:

$$\log M_i = \log M_0 + \frac{A\Delta T}{B + \Delta T} \qquad (1)$$

where M_i and M_0 are MM of a polymer homologue and a Kuhn segment, A and B are coefficients, $\Delta T=T_f-T_g$ (for amorphous) or $\Delta T=T_f-T_m$ (for crystalline) polymer region, respectively. The ΔT is time-dependent property, but temperatures of the glass transition and the beginning of flow depend on frequency or time differently [65, 66]. Therefore, the ΔT value is not preserved constant for the material. However, for TMA measurements, it could be assumed to be independent on a rate and time of loading. It is because under testing conditions, the loading is small and stable, and the scanning rate of temperature is constant, what make some, but small error of evaluation of MM. Under these conditions, MM~M_{min} being directly proportional to $\Delta T_{min}=T_{min}-T_g$ is the lowest MM of chain segments between the branching junctions in a polymer network, which start to flow in a loaded specimen at the temperature T_{min}. The temperature of the beginning of the plateau of high-elasticity, T_∞, is defined as the beginning of stabilization of a thermal expansion rate for the highest MM segments; consequently MM~M_{max} is directly proportional to $\Delta T_{max}=T_\infty-T_g$.

In Fig. 3, the results of TMA testing for polypropylene [67] transformed to new coordinates and our experimental data are collected. It was calculated that $\log M_0$= 2.3, which is almost the same as that ($\log M_0$=2.0) reported earlier [26]. The data in Fig. 3 also confirm A=11 and B=100 empirical coefficients [44] valid for the T_f value obtained from TMA measurements (T_f^{TMA}) and allow to rewrite Eq. (1) as follows:

$$\log M_{min}=2.3+(11\Delta T)/(100+\Delta T)\approx 10^4 \qquad (1a)$$

The response of T_f to the applied load depends, among other factors, on polydispersity of the polymer, its branching degree, and variation in the length

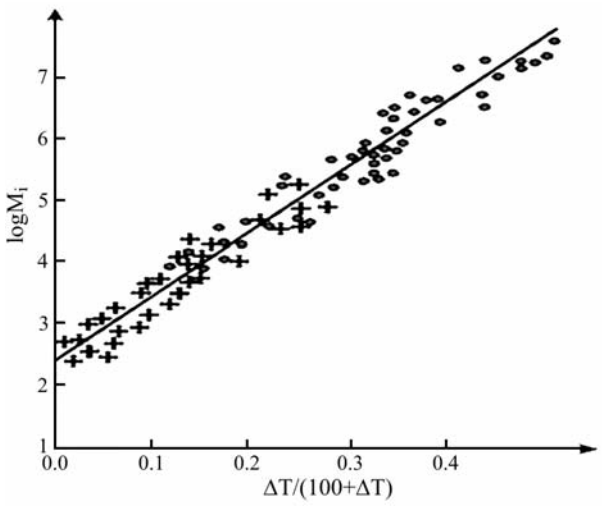

Fig. 3 Correlation chart $\log M_i$–$\Delta T/(100+\Delta T)$; × – corresponds to the molecular mass with short chain homologues and ● – corresponds to the molecular mass with long chain homologues for the same kind of polymer

of branches. Equation (1) has been elaborated for amorphous polymers, but if it is applied for crystalline one, the T_m must be used instead of T_g. For linear polymers with flexible chains T_g and T_m are close to T_∞. It should be mentioned that T_f^{TMA} for the lowest MM polymer homologue is evaluated accurately enough, but it has a relative value for the highest MM. For the latter case, neither a clear end of the segmental relaxation of all chains, nor the beginning of flow of the whole polymer was observed.

In order to verify the usability of this method, experiments have been performed on model linear macrodiisocyanates and respective cross-linked polytriisocyanurates [68]. These macrodiisocyanates according to GPC measurements had: the first $\overline{M}_n$ = 1100 g mol^{-1}, $\overline{M}_w$ =1650 g mol^{-1} and polydispersity index K=1.50, and the second $\overline{M}_n$ =9500 g mol^{-1}, $\overline{M}_w$ =12 300 g mol^{-1}, and K=1.30. They were cross-linked by end-groups according to the triisocyanurate mechanism. After cross-linking, the obtained polymers had the following molecular properties evaluated by the TMA; for the first one, $\overline{M}_{n(n)}$= 1250 g mol^{-1}, $\overline{M}_{n(w)}$=1660 g mol^{-1}, and K=1.33, and for the second one, $\overline{M}_{n(n)}$ =10 100 g mol^{-1}, $\overline{M}_{n(w)}$ = 13 000 g mol^{-1}, and K=1.29. The results obtained are close to each other, which preliminarily suggest the usability of the TMA for evaluation of polymers MMD.

Topological structure

Linear polymers (pseudo-networked system)

Characteristics of the topological structure could be evaluated from TMC, obtained in a standard way.

This structure is represented by the regions differing in both the thermal expansion properties and MMD of the chain segments between junctions of the regions' network. It is assumed that regions represent an effect of interactions that exist in a polymer on its thermal properties and deformability. Therefore, topological regions differ in the molecular mobility and they are related to T_g or T_m.

The ratios of topological regions vary during processing and depend on the filler content and compounding conditions. At least two amorphous regions with the transition temperatures often below 0°C (called a low-temperature region or soft amorphous fraction, SAF) and higher by up to 200°C (called a high-temperature region or a rigid amorphous fraction, RAF) are usually observed. It is postulated that amorphous regions have a structure with physical junctions creating a pseudo-network.

- SAF consists the most mobile chain segments. Physical junctions there are formed by RAF, by other chain segments, which do not strongly interact with the surface of active filler, or by unstable micro(nano?)crystals of a size about critical, because they reduce the mobility of chains.
- RAF consists of chain segments, which interact strongly with crystals, the surface of active filler, zones of interaction with more polar structures in the polymer. The latter creates carbon-black-free cluster type junctions between segments of the chains as all of these essentially reduce the mobility of the chains. It is metastable and consists of, at least, three types of phases having very small dimensions [52, 69]. Sometimes a very small fraction of crystallinity (5%) could freeze all of the remaining amorphous phase into RAF, which is stable only at low temperature [70] equals to high-temperature transition, T_{htt}.
- A crystalline portion consists of the most ordered part of segments of the chains, also interacting with active sites of the carbon black surface (if present).

Every amorphous region could be in three physical states: rigid, rubbery and the plateau of high-elasticity typical for polymers [71]. The third physical state of RAF is flow.

The more sensitive measurements by TMA, the larger number of regions can be found in the polymer. They could be determined not only by segment length (macro-, micro-, or nanophases separation), order (amorphous, mesophases, or crystal), and mobility (glassy, liquid, or mobile mesophases), but also by strong interaction across the phase boundary.

The ratio of thermal expansion coefficients below and above T_g (when changes the mechanism of relaxation) at the same heating rate for unfilled polymers $\alpha_2/\alpha_1 \leq 5.12$ could be accepted as a preliminary indicator of amorphous structure [72], where α_2 is the coefficient of linear thermal expansion in a rubbery state and α_1 is that in a glassy state. It is because the magnitude of α_2/α_1 depends on energy of interchains interaction and energy distribution that dependent on degree of chains order and a share of voids. From TMA measurements $\alpha_1=(\Delta H/H_0)/\Delta T$, where $\Delta H/H_0$ is the relative change in the initial height H_0 (specimen thickness) within the temperature interval ΔT.

A zone *CD* on TMC (Fig. 2) is usually long enough to determine accurately the slope of the straight-line segment of the curve characterizing α_2. If the *CD* zone is short, we can assume that it describes a small amount of the amorphous portion. Then a value of α_2/α_1 roughly determined is usually between 2.5 and 3. However, this interpretation needs additional information from independent sources on the amorphous structure observed.

The crystalline phase contains flexible chain segments of typically 1–100 μm length accommodated into micro- and nanophases. This phase is connected by the passing chains to the amorphous phase via a mesophase due to the frequent crossing of the interface by the long chains. This broadens the glass transition to higher temperature [52] and could cause a separate glass transition for RAF [73]. RAF may lose its solid character below the melting region of the surrounding crystals, within the melting region, or even above the T_f value [69, 74].

TMA is unable to detect crystal form and to evaluate a size of crystalline cell. However, analyzing melting temperatures of different crystalline portions it is possible to make very preliminary conclusions about their amount. The crystalline portion is often composed of several structures differing in the melting temperatures. The crystals are often of lamellar morphology with 5–50 nm in thickness [52]. Wunderlich advanced an idea that the crystalline part of the partially devitrified chain could be treated as a crystalline nanophase in contact with the melt, but decoupled from its reversibly melted ends, which periodically become part of the amorphous phase. The equilibrium between a crystal and a melt can be maintained, as long as the molecular nucleus has a higher melting temperature than that reached by the modulation at DSC test and is retained indefinitely [52].

The frozen gel-like structure is metastable only up to T_g. Once this T_g was reached, further crystallization is possible with the cold-crystallization mechanism, likely producing now different RAF, metastable at high temperature. A size of mesophase could be smaller than that for the crystal phase. In many cases, a mesophase has nanometer size dimensions [52]. It is logical to assume that packing density of the mesophase is intermediate between those of SAF and the

crystalline regions. The crystalline materials are characterized by a ratio of $\alpha_2/\alpha_1>6.24$ [72]. The values $5.12>\alpha_2/\alpha_1>6.24$ characterize structures intermediate between crystalline and amorphous. It means that these structures could be mobile mesophases.

Not all is clear in explanation the variation in crystallinity degree evaluated by different techniques [19], but some correlation between crystallinity degree evaluated by TMA and polymer density exists, Table 1. Some authors assume that a difference between the DSC and TMA results from sensitivity of the latter to aggregated crystals only, but not to micro- and nano-size crystals [75].

Table 1 Comparison of crystallinity degree and polymer density for PA6

Method	Cooling rate/K min^{-1}		
	2 000	100	2
TMA	0.080	0.360	0.770
Polymer density/g cm^{-3}	1.092	1.103	1.151

In high-density polyethylene, the mesophase could be of about 4.0 nm in size when a crystalline lamellar thickness of 25–30 nm [76]. Lower MM and better-crystallized polymers have thinner mesophases, and solution grown crystals may have only 0.2–0.7 nm thick mesophases without the interface that defines the end of the well-ordered crystal [77]. The existence of oriented mesophases, located between the crystalline and amorphous phases, was shown to be the major contributor to the ultimate strength of PET fibers [78–80]. RAF after devitrification is mobile, but it still is not identical in the mobility to the liquid bulk phase, it remains under strain from the strong coupling with the crystal phase across the interface [52].

The above idea of a topological structure of polymers is based on TMA investigations [26, 27, 44] and is similar to that formulated later by Chen and Wunderlich [6, 81] who based mainly on TMDSC or Danch [23–25] who based on DSC, DETA and DMTA. In the mentioned studies, the amorphous regions or fractions have their own characteristics, because they could influence substantially the polymer usage properties.

Cross-linked polymers

Cross-linked polymers can exhibit a similar topological structure as the above-mentioned. However, both SAF and RAF can be networked with cross-links and/or cluster type physical junctions. RAF becomes visible on TMC when the mobility of the chain segments begins to devitrify. It becomes invisible when the thermomechanical deformation reaches the plateau of high-elasticity. Further increase of the temperature is followed by thermal degradation of the network, which is identified as a material decomposition.

Load applied during TMA tests of cross-linked polymers is larger than that for the linear ones. Consequently, it influences the thermomechanical deformation [82–84] and the related effective coefficient of thermal expansion. Cross-linked rubbers fulfill condition, $\alpha_2/\alpha_1<5.12$, according to the above assumption, they are amorphous.

Cross-link density

Two classical methods of evaluation of the effective cross-link density, ν_e, elaborated by Flory and Rehner [85] and by Cluff *et al*. [86] are known. These methods are based on equilibrium of specimen swelling in solvent. For an arbitrarily chosen polymer-solvent system, some uncertainty always exists in the evaluated cross-link density because the polymer-solvent interaction parameter, χ, depends on the ν_e value. It is resulted from a fact that low-energy physical interactions of pseudo-networks and fractions of the stretched chain segments, being out of control, between branching junctions can break irreversibly during swelling, always reducing the ν_e value differently.

Mooney and Rivlin suggest evaluation of ν_e without pre-swelling of the polymer [87, 88]. The here discussed version of TMA also belongs to methods, as that elaborated by Cluff *et al*., which are based on the evaluation of E_∞, and calculation of ν_e using the equation:

$$\nu_e = E_\infty / 3RT \qquad (2)$$

where E_∞ is the equilibrium of high-elastic modulus, R is the universal gas constant, and T is the temperature.

Experiments confirm that ν_e is related to E_∞ by Eq. (2) only if temperature of this modulus determination corresponds with the plateau of high-elasticity [89, 90] when the total degradation of the physical branching junctions in a polymer pseudo-network occurs.

TMC cannot be used directly for evaluation of E_∞ because the measured effective deformation is resulted mostly from two components: the deformation under the applied load (reducing the specimen height) and the thermal expansion (increasing the height) at the plateau of high-elasticity. However, to minimize the error of E_∞ evaluation, because of a relaxation nature of deformation, it is required a constant rate of temperature scanning. It is assumed that the rubbery state begins at T_g (or T_m) in point *B*' (Fig. 4). Usually the Hertz equation is used [91] to evaluate E_∞ from the H_∞ measurements:

$$E_\infty = \frac{3(1-\mu^2)P}{4R_0^{1/2}H_\infty^{3/2}} \quad (3)$$

where μ is the Poisson's ratio, P is the load, and R_0 is the radius of the hemispherical tip of the probe; usually this radius is in the range between 1 and 2 mm. The evaluation of the cross-link density is done by Eq. (4) below obtained [27] by the substitution of Eqs (2) to (3).

$$\nu_e^{TMA} = \frac{(1-\mu^2)P}{4R_0^{1/2}H_\infty^{3/2}RT_\infty} \quad (4)$$

Poisson's ratio for rubbers and many amorphous polymeric materials is about 0.5; therefore, Eq. (4) can be transformed as follows:

$$\nu_e^{TMA} = \frac{0.2P}{R_0^{1/2}H_\infty^{3/2}RT_\infty} \quad (5)$$

Numerous tests were performed to check the adequacy of this equation giving comparable results [92]. Irrespective of the scanning rate of temperature between 0.6 and 40 K min^{-1}, H_∞, $\delta T=T_\infty-(T_g$ or $T_m)$, and ν_e^{TMA} values are virtually constant suggesting that the deformation processes in the transitional zone exhibit a pseudo-equilibrium nature [45].

The polymer deformation, H_∞, at a temperature within a plateau of high-elasticity is directly proportional to the $P^{2/3}$ value and determines the cross-link density. The plateau of high-elasticity corresponds to the equilibrium state at arbitrary conditions of polymer deformation (different loads and scanning rates of temperature). This also means a reversible deformation in this part of TMC, when residual deformation is absent after removing the load applied earlier to the specimen at $T\geq T_\infty$ (dilatometric conditions). Here, TMC is easily transformed to a dilatometric curve.

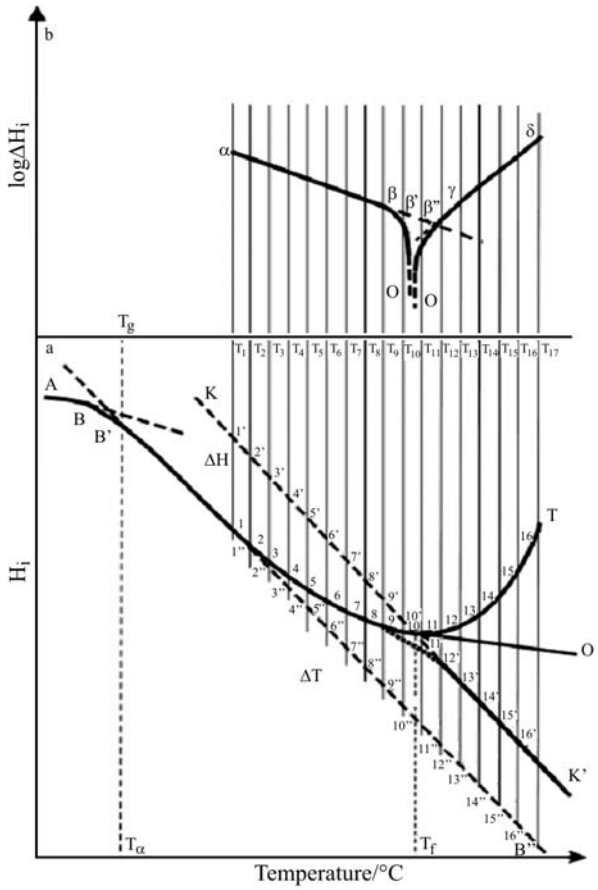

Fig. 4 Exemplary thermomechanical curves of the linear (*A–B–O–T*) and cross-linked (*A–B–O–K*') polymers; *A–B* – glassy state, *O–T* – fixed flow of linear polymer, *O–K*' – rubbery state of a cross-linked polymer in co-ordinates; a – H_i–T and b – logΔH_i–T

Other structural aspects

Structure of networking junctions

At least, chemical (covalent, ionic) bonds between neighboring chains giving cross-links, physical (localized on associated polar groups) resulted from physical interactions, and topological branching junctions created by entangled adjacent high-MM segments of chains can coexist simultaneously in polymer networks [93, 94].

Investigations of low cross-linked polymers show an anomalous magnitude of the ratio of α_2 measured at an arbitrary load to such α_2 measured at 0.1 g (Fig. 5) and termed α_2'. It could be caused by a presence of interlacing junctions. Relaxation of deformation caused by a load P as temperature increases, can result from slipping the chains one against another in the zone of their interlacing, thus reducing the elastic modulus. This increases deformation and lowers α_2' value accordingly. This hypothesis has been proved by synthe-

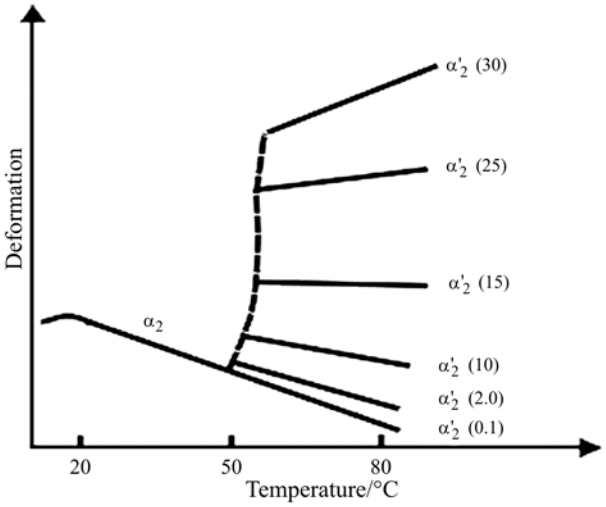

Fig. 5 Combined fragments of TMC obtained at different loading shown in brackets (in g)

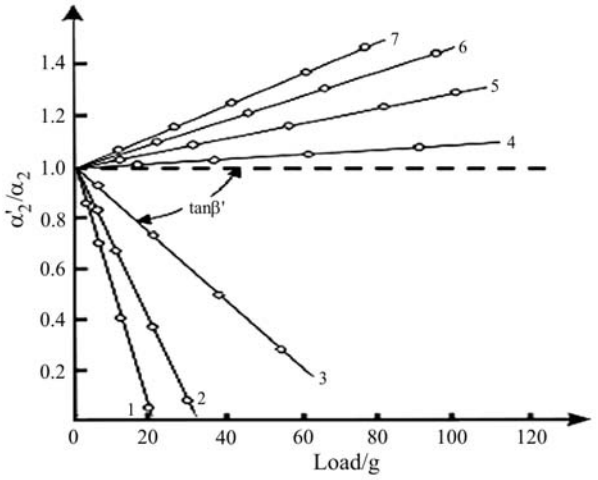

Fig. 6 Dependency of the ratio of coefficients of linear thermal expansion α'_2/α_2 on loading P for the networks containing different quantity of topological interlacing junctions (numbers of curves correspond to Table 2)

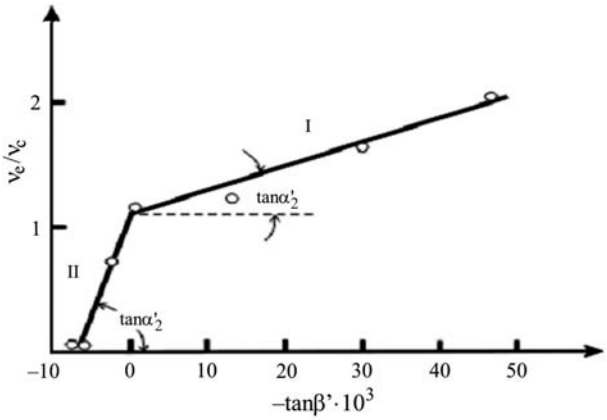

Fig. 7 Dependency of the coefficient of linear thermal expansion on tanβ'; ν_e – effective cross-link density equal to the total concentration of the branching junctions and ν_c – calculated concentration of the branching junctions

sis of the cross-linked polyurethane that based on a copolymer of tetrahydrofurane and propylene oxide, as well as 1,2,3-trimethylopropylene as the branching agent, in which MM of segments between branching junctions was varied. The analysis of ν_e shows that the higher $\overline{M}_{n(n)}$, the more substantial is the difference between the calculated and evaluated values. These calculations have been conducted in terms of the concentration of the branching agent introduced during synthesis. Empirical data (Fig. 6) show that as the share of the topological interlacing junctions rises, so varies the tangent of the inclination angle β' (relative rate of changes in α value on a load P taken in grams) of the straight lines in Eq. (6):

$$\frac{\alpha'_2}{\alpha_2} - 1 = P \tan \beta' \qquad (6)$$

The value of β' (Table 2) has lowered up to zero for equal shares of junctions of different types. Further increase in the concentration of interlacing junctions changes the sign from (–) to (+) and the tanβ' grows. The expression $\nu_e/\nu = f(\beta')$ is the calculated cross-linking density) shown in Fig. 7 reflects two virtually straight lines crossed at tanβ'=0. The empirical relationships between α'_2, α_2, P and the share of topological junctions, φ_t, for the discussed network are as follows:

$$\varphi_t^{I} = 0.5 - 0.045\left(\frac{\alpha'_2}{\alpha_2} - 1\right)P^{-1} \qquad (7)$$

It is valid for $\alpha'_2 < \alpha_2$ for every P-value, and

$$\varphi_t^{II} = 0.5 - 0.0065\left(\frac{\alpha'_2}{\alpha_2} - 1\right)P^{-1} \qquad (8)$$

This implies the presence there equal shares of different types of junctions differing in degradation energy. Each straight line can be treated as independent relationship for the networks, which are characterized by $\alpha'_2 < \alpha_2$ (the curve I for the networks with low cross-link density ν_e and consequently lower interaction energy that resistance the thermal expansion) and by $\alpha'_2 > \alpha_2$ (the curve II for those with high ν_e and consequently higher interaction energy that resistance the

Table 2 Content and properties of cross-linked polyurethanes based on copolymer of tetrahydrofurane and propylene oxide, as well as 1,2,3-trimethylpropylene as the branching agent

No.	ρ_3	$\nu \cdot 10^4$/mol cm^{-3}	$\nu_e \cdot 10^4$/mol cm^{-3}	ν_e/ν	tanβ'·10^3
1	0.013	0.195	0.56	3.08	–46.0
2	0.024	0.36	0.95	2.64	–30.0
3	0.039	0.59	1.34	2.27	–13.0
4	0.054	0.81	1.76	2.17	0.83
5	0.077	1.16	1.97	1.70	2.86
6	0.143	2.15	2.20	1.02	5.29
7	0.200	3.00	3.10	1.03	6.25

ρ_3 is the share of hydroxyl groups in the branching agent, ν is the calculated cross-link density, $\nu = 5 \cdot 10^{-4}$ [OH]$_3$, where [OH] is concentration of hydroxyl groups in the branching agent

thermal expansion). It is valid for $\alpha_2'>\alpha_2$ and for every *P*-value. For $\alpha_2'=\alpha_2$ the shares of topological junctions and cross-links are equal to 0.5, α_2' is α_2 for P=0.1 g, and P is loading the probe (in g).

The following empirical expressions are generally accepted [28, 95, 96]:

$$3(\alpha_2-\alpha_1)T_g=0.12 \text{ or } 0.113 \quad (9)$$

and

$$3\alpha_2 T_g=0.2 \quad (10)$$

These dependencies imply that interactions expressed by T_g are correlated with those expressed by thermal expansion coefficient. Combining these equations, we obtain:

$$\alpha_2/\alpha_1=2.5 \quad (11)$$

From experiments it could be preliminarily concluded that the network has branching junctions of chemical nature if $6>\alpha_2/\alpha_1\geq 2.5$. For $\alpha_2/\alpha_1<2.5$ the network has junctions of complex (chemical, physical and topological) nature [97]. However, this conclusion should be confirmed by further studies.

The share of the topological interlacing junctions φ_t can be found from Eq. (12) assuming that under testing conditions only cross-links and topological branching junctions are present in rubber.

$$\varphi_t=1-\varphi_c \quad (12)$$

where $\varphi_c=\nu_c/(\nu_c+\nu_t)$ is the share of cross-links and cluster type junctions. However, this condition not often is fulfilled.

Anisotropy of a structure

To evaluate the anisotropy in local properties resulted form distribution of super molecular structures, TMC should be recorded in two perpendicular directions. A measure of anisotropy could be the ratio of the amount of crystalline portion, K_a, particularly in parallel (φ^{II}) and perpendicular ($\varphi^{\perp}$) direction to that used in specimen obtained by compression molding.

$$K_a=\varphi^{II}/\varphi^{\perp} \quad (13)$$

As mentioned above, TMA evaluates usually polymer properties in a layer up to 0.5 mm thick, but if the radius of the probe tip is increased from 1 to 5 mm, this thickness grows up to 2.5 mm. Because of this, the properties measured by using a probe tip equal to 1 mm in two perpendicular directions on a small specimen differ also due to another material area tested. It suggests using for anisotropy evaluation a radius of a probe tip about 5 mm when the tested area could be similar.

Compactness

Compactness is determined by a volume of voids within material, but it depends substantially on methodology used for its evaluation. The thermal expansion coefficients could be used to evaluate the compaction factor, V_c^{TMA}, for amorphous polymers using the following empirical expression:

$$V_c^{TMA}=3(\alpha_2-\alpha_1)T_g \quad (14)$$

where T_g is taken in Kelvin scale.

In Eq. (14), it is accepted that volumetric thermal expansion coefficient equals to three linear one, what is equal with presumption that material is isotropic and sizes of voids are similar in three Cartesian directions. This dependence has been elaborated for polymers in iso-free state usually being a non-fulfilled condition. The V_c^{TMA} varies for a particular polymer depending on its molecular mass, cross-linking degree, rigidity of the chains, and conditions of its structure formation. The V_c^{TMA} is related with compactness in nano-, micro-, and macro-scale as well as a free volume fraction, shares of which depend on technology of specimen manufacturing. For linear soft-chain polymers in amorphous state $V_c^{TMA}\approx 0.113$ [98], whereas for rigid-chain polymers, which tend to form crystalline structures it is below 0.113. For polymer composites $V_c^{TMA}>0.113$ implying their less compact structure. Because of the material structure heterogeneity, including a non-uniform distribution of voids within the specimen and distribution of sizes of voids observed, the V_c^{TMA} depends on a point of measurements. Simultaneously, it is needed to consider that the distribution of voids within a polymeric material is not uniform and allows different motions [99]. A particular T_g can correspond to different statistical distributions of voids caused by variations in the structure.

Conclusions

The TMA offers potential possibilities for the study some aspects of the molecular and topological structures of linear, cross-linked, and filled polymeric materials. Some characteristics of the topological regions evaluated from TMA correlate satisfactory (r>0.7) with the static and dynamic mechanical properties of rubbers and plastics [68], but the strength of correlation depends on which characteristics have been compared, and on rubber formulation. This suggests a substantial influence of a structure of the branching junctions of a polymer network on correlation between characteristics of the topological and molecular structures of polymeric material from TMA and its mechanical properties. Such correlation implies that it is reasonable studying other materials to explain variations

in properties resulted from material formulation and processing conditions, and to optimize the polymer compounding and processing technologies. However, any model approach involves idealization of certain properties of a system, while some other properties are not taken into account at all. Only judging from its application to solve relevant problems one can assess the validity of this approach. It would be very important to outline the limits of usability of TMA for multi-aspect description of the polymeric systems.

Appendix

E_∞	equilibrium of a high-elastic modulus
H	specimen deformation
H_0	height of the specimen
H_∞	equilibrium of a high-elastic deformation
K	polydispersity index
M_i	molecular mass of a polymer homologue
M_{min}	the lowest molecular mass of chain segments between junctions in the polymer network or pseudo-network, which start to flow in the loaded specimen at temperature T_{min}
M_{max}	the highest molecular mass for chains, which start to flow in the loaded specimen at T_∞
M_0	molecular mass of Kuhn segment
$\overline{M}_{n(n)}$	number-average molecular mass of the chain segments between junctions of networked and/or pseudo-networked polymer
$\overline{M}_{n(w)}$	mass-average molecular mass of the chain segments between junctions of networked and/or pseudo-networked polymer
P	load applied on the probe
R	universal gas constant
R_0	radius of the hemispherical tip of the probe
T	temperature
T_f	temperature of the beginning of a flow or 'sol state'
T_g	temperature of the glass transition
T_{htt}	temperature of the high-temperature transition
T_m	temperature of the beginning of melting process
T_∞	temperature of the beginning of the plateau of high-elasticity
V_c^{TMA}	compaction factor
ΔH	deformation jump or deformation of the specimen
α_1	coefficient of linear thermal expansion in a glassy state
α_2	as α_1 but in rubbery state
α_2'	α_2 for load of 0.1 g
α_{cr}	coefficient of the thermal change in linear dimensions during melting
φ_c	share of chemical and cluster type junctions
φ_t	share of topological junctions
χ	interaction parameter
μ	Poisson's ratio
ν	calculated cross-link density
ν_e	effective cross-link density
ν_t	share of topological junctions

Abbreviations

DETA	dielectric thermal analysis
DM(T)A	dynamic mechanical (thermal) analysis
(TM)DSC	(thermally modulated) differential scanning calorimetry
MM	molecular mass
MMD	molecular mass distribution
RAF	rigid-amorphous fraction or a high-temperature amorphous region
SAF	soft amorphous fraction or a low-temperature amorphous region
TMA	thermomechanical analysis
TMC	thermomechanical curve

References

1 P. J. Flory, Principles of Polymer Chemistry, Cornell University Press, Ithaca, NY 1953, p. 422.
2 P. J. Flory, Statistical Mechanics of Chain Molecules, Interscience Publishers, New York–London–Sydney–Toronto 1969; Russian translation Mir, Moscow 1971.
3 B. Wunderlich and J. Grebowicz, Adv. Polym. Sci., 60 (1984) 1.
4 G. W. Gray, Molecular Structure and Properties of Liquid Crystals, Academic Press, New York 1962.
5 B. Wunderlich, M. Moeller, J. Grebowicz and H. Baur, Advances in Polymer Science, Vol. 87, Springer, Berlin 1988.
6 W. Chen and B. Wunderlich, Macromol. Chem. Phys., 200 (1999) 283.
7 B. Wunderlich, Prog. Polym. Sci., 28 (2003) 383.
8 S. D. Gehman, Rubber Chem. Technol., 40 (1967) 532.
9 V. V. Yevreinov, Y. G. Tkach and S. G. Entelis, Vysokomol. Soed., A15 (1973) 936.
10 V. V. Zabrobein, V. I. Zikov and G. I. Chui, Vysokomol. Soed., B15 (1973) 678.
11 M. Mayen, Eur. Polym. J., 22 (1986) 987.
12 J. G. Curro, J. Polym. Sci., Polym. Phys., 14 (1976) 177.
13 M. Baba, J. L. Gardette and J. Lacote, Polym. Degrad. Stab., 65 (1999) 415.
14 N. N. Volkova, G. I. Sandakov, A. I. Sosikov, Y. A. Olkhov, L. P. Smirnov and K. T. Sumanen, Vysokomol. Soed., A34 (1992) 77.
15 Y. A. Olkhov, V. I. Irzhak and S. M. Baturin, Proc. of the First Europ. East-West Symp. Mater. and Proc. Helsinki, 1990, p. 220.
16 V. I. Irzhak, Usp. Khim., 69 (2000) 780.
17 L. J. Fetters, D. J. Lhose, C. A. Garcia-Franco, L. P. Braun, and D. Richter, Macromolecules, 35 (2002) 10096.
18 W. Thimm, C. Friedrich, M. Marth and J. J. Honerkamp, Rheol., 45 (2001) 604.
19 R. S. Anderssen and D. W. Mead, J. Non-Newtonian Fluid Mech., 76 (1998) 299.
20 G. V. Vinogradov, E. A. Dzura, A. Y. Malkin and V. A. Grechanovskii, J. Polym. Sci., A2 (1971) 1153.
21 Y. I. Matveev and A. A. Askadskii, Vysokomol. Soed., A35 (1993) 63.
22 B. Baumgartel, A. Schausberger and H. H. Winter, Rheol. Acta, 29 (1990) 400.

23 A. Danch, J. Therm. Anal. Cal., 54 (1998) 151.
24 A. Danch, J. Therm. Anal. Cal., 56 (1999) 1097.
25 A. Danch, A. Kocot, J. Ziolo and F. Stelzer, Macromol. Phys. Chem., 202 (2001) 105.
26. Y. A. Olkhov, V. I. Irzhak and S. M. Baturin, RU Patent 1763952 A1 (27 Oct. 1989).
27 Y. A. Olkhov, V. I. Irzhak and S. M. Baturin, RU Patent 2023255 (27 Oct. 1989).
28 R. F. Boyer, Rubber Chem. Technol., 36 (1963) 1303.
29 B. Wunderlich, Thermal Analysis, Academic Press, New York, NJ 1990.
30 J. Zielnica, P. Wasilewicz, B. Jurkowski and B. Jurkowska, Thermochim. Acta, 414 (2004) 255.
31 V. V. Tsukruk, V. V. Gorbunov and N. Fuchigarni, Thermochim. Acta, 395 (2003) 151.
32 J. Wolfrum, G. W. Ehrenstein and M. A. Avonder, J. Therm. Anal. Cal., 56 (1999) 1147.
33 W. Brostow, E. A. Faitelson, M. G. Kamensky, V. P. Korkhov and Y. P. Rodin, Polymer, 46 (1999) 1441.
34 S. S. Vatalis, A. Kanapitsas, C. G. Delides and P. Pissis, Thermochim. Acta, 372 (2001) 33.
35 S. S. Vatalis, C. G. Delides, G. Georgoussis, A. Kyritsis, O. P. Grigorieva, L. M. Sergeeva, A. A. Brovko, O. N. Zimich, V. I. Schtompel, E. Neagu and P. Pissis, Thermochim. Acta, 371 (2001) 87.
36 C. S. Wang and T. S. Leu, Polymer, 41 (2000) 3581.
37 S. H. Hsiao and C. T. Li, J. Polym. Sci., Polym. Chem., 37 (1999) 1435.
38 C. Konetschny, D. Galusek, S. Reschke, C. Fasel and R. Riedel, J. Eur. Ceram. Soc., 19 (1999) 2789.
39 Y. I. Matusevich, A. P. Polikarpov and L. P. Krul, High Energ. Chem., 33 (1999) 224.
40 A. Pizzi, R. Garcia and J. Wang, J. Appl. Polym. Sci., 66 (1997) 255.
41 C. Tonin, A. Algi, M. Binchetto Sognia, C. D'Arrigo, M. Mormino and C. Vineis, J. Therm. Anal. Cal., 77 (2004) 987.
42 T. F. Irzhak, S. E. Variukhin, Y. A. Olkhov, S. M. Baturin and V. I. Irzhak, Vysokomol. Soed., A39 (1997) 671.
43 D. Stauffer, A. Conoglio and M. Adam. Adv. Polym. Sci., 44 (1982) 74.
44 Y. A. Olkhov and B. Jurkowski, J. Appl. Polym. Sci., 65 (1997) 499.
45 B. Jurkowska, Y. A. Olkhov and B. Jurkowski, J. Appl. Polym. Sci., 74 (1999) 490.
46 Y. A. Olkhov, S. M. Baturin and V. I. Irzhak, Polym. Sci. (Russia), A38 (1996) 849.
47 V. A. Bershtein and V. M. Egorov, Differential Scanning Calorimetry in the Physical Chemistry of Polymers (in Russian), Khimia, Leningrad 1990.
48 W. G. Rostiashvily, V. I. Irzhak and B. A. Rozenberg, Glassing of Polymers (in Russian), Khimia, Leningrad 1987.
49 D. W. Van Krevelen, Properties of Polymers: Correlation with Chemical Structure, Elsevier, Amsterdam 1972.
50 B. Wunderlich, Macromolecular physics, Crystal structure, morphology, defects, Vol. 1, Academic Press, New York 1973; B. Wunderlich, Macromolecular physics, Crystal nucleation, growth, annealing, Vol. 2, Academic Press, New York 1976; B. Wunderlich, Macromolecular physics, Crystal melting, Vol. 3, Academic Press, New York 1980.
51 J. Pak, M. Pyda and B. Wunderlich, Macromolecules, 36 (2003) 495.
52 B. Wunderlich, Prog. Polym. Sci., 28 (2003) 383.
53 A. Danch, W. Osoba and F. Stelzer, Eur. Polym. J., 39 (2003) 2051.
54 A. Danch and W. Osoba, J. Therm. Anal. Cal., 72 (2003) 641.
55 A. Danch, Fibres & Textiles in Eastern Europe, 11 (2003) 128.
56 M. E. Solovev, doctoral thesis, Moscow: Institute of Chem. Physics, Russian Academy of Sci., 1994.
57 A. R. Basaev, N. A. Budanov, M. E. Solovev and Y. E. Shapiro, Vysokomol. Soed., B30 (1988) 570.
58 M. E. Solovev, A. B. Raukhvarger, L. I. Makhonina, V. I. Irzhak and G. V. Korolev, Vysokomol. Soed., B31 (1989) 485.
59 A. I. Marei, In: Physical Properties of Elastomers, Khimia, Leningrad 1975; p. 31 (in Russian).
60 M. J. Banach and A. H. Windle, Liquid Crystalline Polymers, Cambridge University Press, Cambridge 1992.
61 M. J. Banach, R. H. Friend and H. Sirringhaus, Macromolecules, 36 (2003) 2838.
62 Y. A. Olkhov, Y. B. Kalmikov and S. M. Baturin, Vysokomol. Soed., A26 (1984) 1681.
63 V. A. Kargin and G. L. Slonimskii, DAN SSSR, 62 (1948) 239.
64 M. L. Williams, R. F. Landel and J. D. Ferry, J. Amer. Chem. Soc., 77 (1955) 3701.
65 K. L. Ngai and D. J. Plazek, Rubber Chem. Technol., 68 (1995) 376.
66 K. L. Ngai and D. J. Plazek, Macromolecules, 35 (2002) 9130.
67 E. E. Alianova, N. M. Bravaya, T. Ponomarieva, V. I. Tsvietkova, P. M. Nedorezova and V. I. Irzhak, Polym. Sci. (Russia), 40B (1998) 345.
68 B. Jurkowska, B. Jurkowski and Y. A. Olkhov, 81 (2005) 27.
69 F. E. Karasz, H. E. Bair and J. M. O'Reilly, J. Polym. Sci., Part A-2, 6 (1968) 1141.
70 S. Z. D. Cheng, R. Pan and B. Wunderlich, Macromol. Chem., 189 (1988) 2443.
71 J. D. Ferry, Visco-elastic Properties of Polymers, Wiley, New York and London 1980.
72 B. Jurkowski, B. Jurkowska and K. Andrzejczak, Polymer testing, 21 (2002) 135.
73 J. Menczel and B. Wunderlich, J. Polym. Sci., Polym. Lett. Ed., 19 (1981) 261.
74 S. Z. D. Cheng and B. Wunderlich, Macromolecules, 20 (1987) 1630.
75 L. V. Adamova, T. Y. Korniakova, A. A. Tager, I. S. Tiukova, V. A. Shershnev, I. K. Shundrina and V. D. Yulovskaja, Vysokomol. Soed., 38A (1996) 1362.
76 J. Cheng, M. Fone, V. N. Reddy, K. B. Schwartz, H. P. Fisher and B. Wunderlich, J. Polym. Sci., Part B: Polym. Phys., 32 (1994) 2683.
77 L. Mandelkern, R. G. Alamo and M. A. Kennedy, Macromolecules, 23 (1990) 4721.
78 Y. Fu, B. Annis, A. Boller, Y. Jin and B. Wunderlich, J. Polym. Sci, Part B: Polym. Phys., 32 (1994) 2289.
79 Y. Fu, W. R. Busing, Y. Jin, K. B. Affholter and B. Wunderlich, Macromol. Chem. Phys., 195 (1994) 803.

80 Y. Fu, W. R. Busing, Y. Jin, K. A. Affholter and B. Wunderlich, Macromolecules, 26 (1993) 2187.
81 B. Wunderlich, J. Therm. Anal. Cal., 78 (2004) 7.
82 I. R. Ladygina, Y. A. Gorbatkina and S. S. Epifanova, Vysokomol. Soed., A12 (1970) 1349.
83 T. I. Ponomarieva, A. I. Efremova, Y. N. Smirnov, V. I. Irzhak, E. F. Olejnik and B. A. Rozenberg, Vysokomol. Soed., A22 (1980) 1958.
84 T. I. Ponomarieva, Y. M. Paramonov, V. I. Irzhak and B. A. Rozenberg, Vysokomol. Soed., B25 (1983) 205.
85 P. I. Flory and I. Rehner, J. Chem. Phys., 11 (1943) 521.
86 E. F. Cluff, E. K. Glading and R. J. Pariser, J. Polym. Sci., 45 (1960) 341.
87 M. Mooney, J. Appl. Phys., 11 (1940) 582.
88 R. S. Rivlin, Phil. Trans. Roy. Soc., A (1948) 241.
89 Y. A. Olkhov and V. I. Irzhak, Polymer Sci. (Russia), 40B (1998) 1706.
90 L. S. Priss, A paper presented at the Second Conference 'Mathematical methods in investigation of Polymers', Pushchino (Russia) 1981, Preprint.
91 J. M. Barton, Analytical Proceedings, 8 (1981) 411.
92 Y. A. Olkhov and Y. I. Estrin, RU Patent, 154 0463 (July 3, 1987).
93 V. M. Litvinov, D. Barendswaard and M. van Duin, Rubber Chem. Technol., 71 (1998) 105.
94 J. E. Mark and B. Erman, Rubber-like Elasticity, A Molecular Primer, John Wiley & Sons, New York 1988.
95 R. Simha and R. F. Boyer, J. Chem. Phys., 37 (1962) 1003.
96 Y. S. Lipatov, Physical Chemistry of Filled Polymers (in Russian), Khimia, Moscow 1977.
97 Y. A. Olkhov, G. A. Gorbushina and S. M. Baturin, RU Patent 1713359 A1 (11 Sept. 1989).
98 A. J. Hill, M. D. Zipper, M. R. Tant, G. M. Stack, T. C. Jordan and A. R. Schultz, J. Phys. Cond. Mat., 8 (1996) 3811.
99 Y. S. Lipatov, Usp. Khim., 47 (1978) 332.

Received: November 30, 2004
In revised form: March 30, 2005

DOI: 10.1007/s10973-005-6517-y